

# Chapter 10

## Wear



Chunming Jin and Wei Wei

### 10.1 Introduction

Wear is a critical issue for prostheses, implants, and other medical devices. Wear may lead to significant loss of material and/or failure of a medical device. For example, wear and wear-related damage commonly cause failure of hip, knee, and other orthopedic prostheses [1]. Even a relatively small amount of wear can lead to significant degradation of function for some medical devices. For example, wear debris generated from degradation of a joint prosthesis can result in a biological process known as osteolysis (bone resorption), which can cause loosening of the prosthesis [2, 3]. Wear may also lead to failure of artificial heart valves and other medical devices that enable critical physiologic activities [4]. In this chapter, the wear mechanisms that are commonly encountered in biomedical materials and medical devices are discussed.

### 10.2 Friction, Lubrication, and Wear

Friction, lubrication, and wear are three concepts that are encountered when examining the relative motion of two surfaces that are placed in contact. The significance of friction, lubricant, and wear in the function of medical devices has been investigated for several decades. The scientific examination of friction, lubrication, and wear emerged as an independent field in the 1960s. For example, the term “tribology”

---

C. Jin (✉)

Department of Biomedical Engineering, North Carolina State University, Raleigh, NC, USA  
e-mail: [cjin@ncsu.edu](mailto:cjin@ncsu.edu)

W. Wei

Department of Materials Science and Engineering, North Carolina State University,  
Raleigh, NC, USA

originated in a 1966 British Department of Education and Science report to describe the study of friction, lubrication, and wear. Soon afterward, Dowson coined the phrase “biotribology” to describe the examination of wear, friction, and lubrication in biological systems [5].

The term friction refers to the resisting force that acts along the surfaces of two interacting bodies. Friction force occurs under the following conditions: (1) there is a force acting perpendicularly to the surfaces, (2) the surfaces have a predisposition toward relative movement or are actively moving relative to each other. Friction force  $F_f$  is related to the normal force  $F_{\perp}$  through the following equation:

$$F_f = \mu F_{\perp} \quad (10.1)$$

in which  $\mu$  is known as the coefficient of friction and is a dimensionless quantity. The friction force between surfaces that are moving relative to each other is referred to as kinetic friction. When there is no relative motion between the two surfaces, a friction force known as static friction is observed; the static friction coefficient is higher than kinetic friction coefficient. Movement of objects leads to energy loss since kinetic energy is converted to thermal energy. Materials known as lubricants may be used to separate the surfaces of the two interacting bodies in order to minimize friction and wear. Gases, liquids, solid films, or particles can serve as lubricants.

Friction is divided into dry friction and viscous friction. The term dry friction refers to friction behavior between two dry sliding solid bodies. Viscous friction refers to friction behavior of solid bodies that are separated by gases or fluids. In ideal situations, classical laws are valid for dry friction. For example, the frictional force is proportional to the normal load in ideal situations. In addition, the coefficient of friction is independent of surface area and sliding speed. Viscous or lubricated friction can be classified into different categories using the Stribeck curve [6, 7], which is shown in Fig. 10.1. The Stribeck curve is a plot of the coefficient of

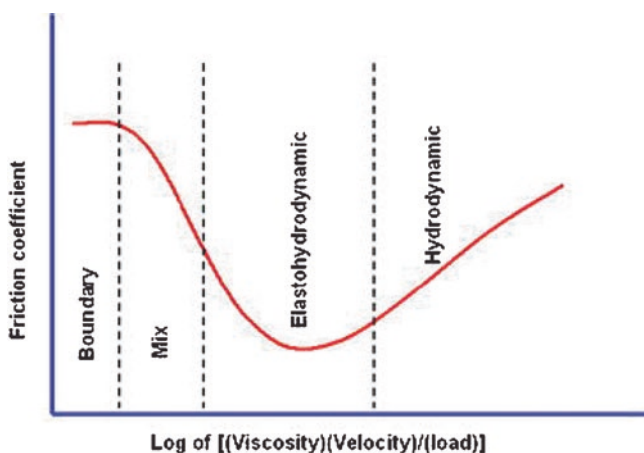


Fig. 10.1 Schematic illustration of the Stribeck curve, which shows different lubrication regimes

friction as a function of the parameter  $ZN/P$ , where  $Z$  is the viscosity of the lubricant,  $N$  is the velocity, and  $P$  is the load. When the value of  $ZN/P$  is low, a thin lubricant film coats the sliding surfaces; this situation is referred to as boundary lubrication. In boundary lubrication, the thickness of the lubricant film is similar to the height of the uneven features (asperities) on the surface of the material. In this case, the coefficient of friction is determined by the chemical properties of the lubricant film, the physical properties of the lubricant film, and the lubricant film thickness; this lubricant film (known as a boundary film) serves to limit wear. In general, boundary lubrication is characterized by relatively high coefficient of friction values and wear rates. A high  $ZN/P$  value corresponds to a situation in which high velocities, high lubricant viscosities, and low loads are observed. In this case, which is known as hydrodynamic lubrication, a thick, continuous lubricant film is observed between the two sliding surfaces. Friction in this regime is determined by the rheologic properties of the lubricant; wear of the sliding surfaces is limited since the two surfaces are not in direct contact. In elasto-hydrodynamic lubrication, the lubricant film is thinner than in hydrodynamic lubrication, but it is sufficiently thick to prevent the two surfaces from directly contacting one another. Elastic deformation of the sliding surfaces may result from transfer of pressure through the separation film. In the mixed lubrication regime, the lubricant film is thin and discontinuous. Direct interaction between the two sliding surfaces occurs, resulting in high wear rates. In this regime, elasto-hydrodynamic and boundary mechanisms may be active at the same time. In large joints, the two sliding surfaces are bones that are covered at the ends with articular cartilage. In a healthy joint, viscous synovial fluid provides a lubricant that is released into the joint space under pressure in what is commonly referred to as “weeping” lubrication. The articulating motion for healthy human joint has very low coefficient of friction, which is in the range 0.005–0.025 [26]. In the human body, different lubrication modes may be observed at various stages of tissue motion. For example, boundary lubrication is the dominant mechanism when joint motion is initiated [8].

The term “wear” covers a wide range of phenomena related to surface damage; it is commonly defined as “damage to a solid surface, generally involving progressive loss of material, due to relative motion between that surface and a contacting substance or substances” [9–11]. Wear damage may also occur by means of plastic deformation near the surface of a material. In this case, no material removal is observed, but the shape of the material is changed due to the relative motion of the two surfaces. Wear damage to the surface of material may include any manner of surface degradation, including material removal, material displacement due to plastic deformation, topology changes (e.g., fracture), and surface chemical changes (e.g., oxidation) [10, 11].

## 10.3 Wear Classifications and Fundamental Wear Mechanisms

Several classification schemes have been developed to understand and compare wear processes. One or more fundamental wear mechanisms may play a role in any given real-world wear process. Wear is classified based on several characteristics, including (1) the physical mechanism by which wear damage occurs, (2) the appearance of the wear damage, and (3) the condition of the wear process [11]. Bayer classified the physical mechanism of the wear damage into eight distinct categories, including adhesive wear, single-cycle deformation wear, repeated-cycle deformation wear, corrosive or oxidation wear, thermal wear, tribofilm wear, abrasive wear, and atomic wear [11]. In many biomedical devices (e.g., artificial joints), damage generally occurs by means of adhesive wear, abrasive wear, corrosive wear, and fatigue wear [1].

### 10.3.1 Adhesive Wear

Adhesive wear originates from adhesion between two surfaces that are placed in contact. When two surfaces are brought into contact, asperities of the two surfaces make physical contact. This “true” contact area is significantly smaller than the apparent surface area of the two contact surfaces. The contact area between the two surfaces is localized to the small regions known as asperities; these asperity-asperity contact regions are referred to as junctions [11]. The size of a junction is usually in the range of 1–100  $\mu\text{m}$ ; the typical size of a junction is 10  $\mu\text{m}$  in diameter. The number of junctions is dependent on the surface roughness and the amount of load that is applied. Under load, bonding between asperities on the two contact surfaces may occur. The amount of deformation at these junctions is also dependent on the number of junctions and the size of the junctions. Under sliding motion, plastic deformation, cracking, and fracture can occur in the “true” contact area. Adhesive wear is largely due to fracture of material and transfer of material at the asperity-asperity contact regions (Fig. 10.2). Prior to fracture, plastic deformation and crack formation may cause damage to the contact surfaces.

The formation of wear debris is dependent on the mechanical properties of the contact materials and the geometry of the asperities on the contact surfaces. For example, ductile materials generally produce a higher number of wear particles than brittle materials. Wear debris is usually generated from the material with lower hardness values. For example, in an orthopedic prosthesis that contains metallic and polymeric components, the adhesive wear debris is usually generated from the polymeric component [12]. Adhesive wear is associated with a high wear rate and a variable coefficient of friction [7, 11, 13].

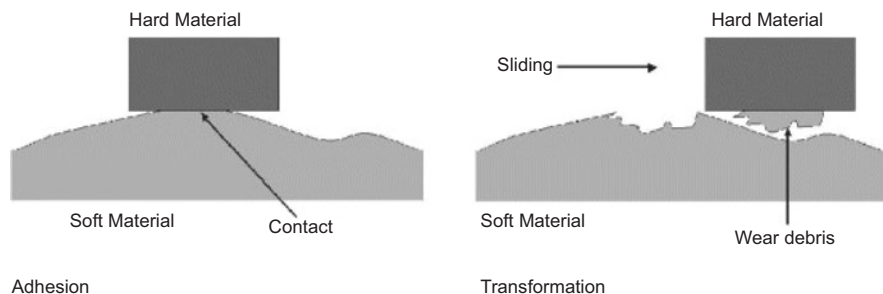


**Fig. 10.2** Schematic illustrations of adhesive wear behavior

The adhesion between two surfaces is also dependent on the chemical properties of the contact surfaces [13]. Materials with similar chemical properties generally exhibit higher adhesive forces because they are able to form chemical bonds more readily. Strong metal-to-metal adhesion may occur as a result of electron exchange and bond formation. For example, when adhesion between iron and other metals was examined under vacuum, the iron-iron contact had the highest adhesive force, and the iron-aluminum contact had the second highest adhesive force [13]. In certain cases, the thin oxide layers on many metallic materials may limit chemical bonding between metal surfaces. Strong adhesion between metallic and polymeric materials is also commonly observed. Adhesive wear is also a significant wear mechanism for joint prostheses that contain metallic and polymeric components. Chemical interaction and adhesive wear has been also observed between metal and ceramic contact surfaces [14].

An equation first proposed by Archard in 1953 has been developed to describe the volumetric wear rate for adhesive wear [11, 15]:

$$R_v = \frac{KP}{3h} \quad (10.2)$$

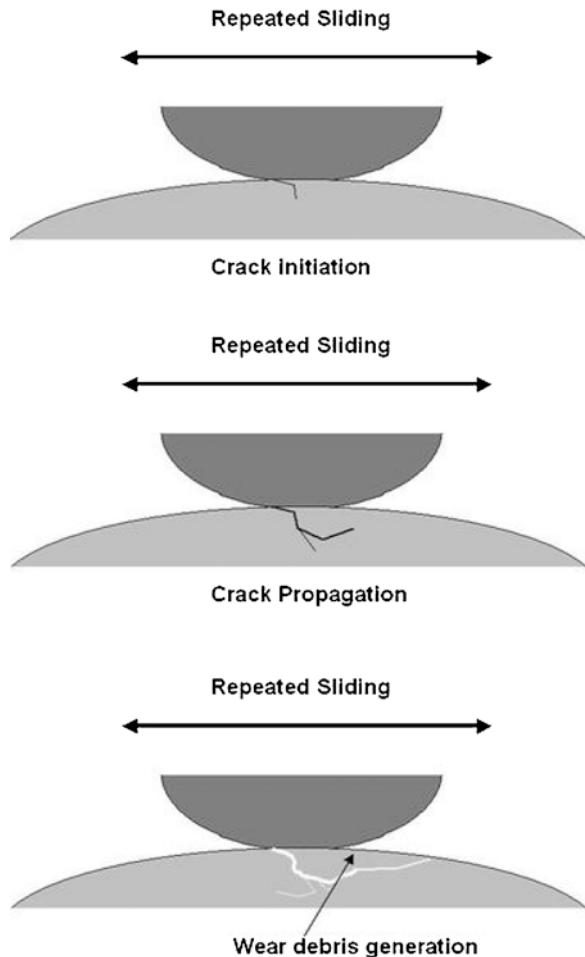
In this equation,  $K$  is the probability that a given junction will produce adhesive wear,  $P$  is the normal force that holds the two contact surfaces together, and  $h$  is the penetration hardness of the softer material. This equation indicates that the adhesive wear rate is directly proportional to the load and inversely proportional to the hardness of the softer material. The equation also indicates that adhesive wear rate is proportional to the value of  $K$ . The value of  $K$  is determined by the adhesive behavior of the junction interface; weaker adhesion is correlated with smaller  $K$  values. For self-mated metals, typical values for  $K$  are in range of  $2 \times 10^{-4}$  to 0.2 for dry wear and  $9 \times 10^{-7}$  to  $9 \times 10^{-4}$  for lubricated wear [16]. This equation provides good agreement with experimental data in most cases.

### 10.3.2 Fatigue Wear

Fatigue wear is a wear mechanism that occurs when a material undergoes cyclic loading. Other wear mechanisms such as delamination wear and flow wear also fall in the general category of repeated-cycle wear processes [11]. Fatigue wear can be observed in sliding, rolling, or impact wear processes. In repeated rolling processes, wear damage may be referred to as surface fatigue or contact fatigue [13].

In repeated sliding situations, fatigue wear may occur even if the coefficient of friction is small and lubricant is present. In this mechanism, shear forces during sliding processes cause strain near the surface. As the plastic strain accumulates, the movement of dislocations leads to the formation of microcracks on the surface or below the surface (Fig. 10.3). Cracks are initially produced on the weak, imperfect, or otherwise damaged regions of the contact surface. These cracks grow and

**Fig. 10.3** Schematic illustration of fatigue wear behavior



propagate through the material to form crack networks under repeated sliding motion. As the two surfaces continue to slide against one another, material on the contact surface is fractured, and wear debris is formed. In rolling contacts, fatigue wear mechanisms depend mostly on the material properties and testing/operational conditions.

### ***10.3.3 Abrasive Wear and Third-body Wear***

Abrasive wear is caused by plowing of particles and asperities [7, 11, 13]. This wear process is commonly observed when the surface is placed in contact with either particles or surfaces that exhibit equal or greater hardness values. The term “abrasion” is commonly used to describe wear processes involving two wearing surfaces, and the term “erosion” is commonly used to describe wear processes in which only one surface is involved. Abrasion processes may be subdivided into two-body and three-body abrasion processes [11]. Two-body abrasion involves damage caused by the particles and asperities that are attached to another surface. On the other hand, three-body abrasion wear process involves damage caused by hard particles that are not fixed on a surface but instead move between the two contact surfaces.

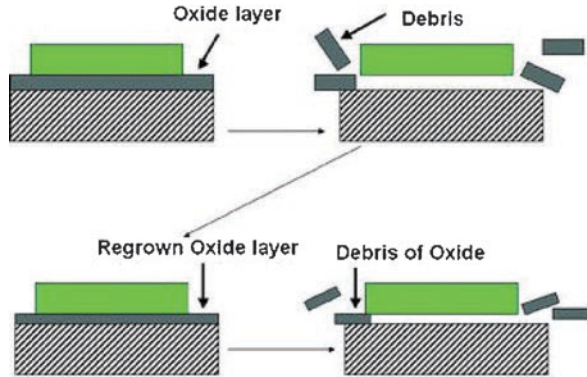
Abrasive wear can occur through four types of mechanisms: cutting, fracture, fatigue, and grain pullout [13]. The cutting mechanism occurs when a hard sharp particle or surface asperity ploughs into the surface of the softer surface. Surface damage can also occur by fracture of brittle material, fatigue under repeated deformation, and grain detachment due to sliding of abrasive particles.

For ductile materials, abrasive wear volume is proportional to the normal load and the sliding distance and is inversely proportional to the hardness of the material [8]. For brittle materials, wear debris is produced primarily as a result of fracture. In this case, the abrasive wear rate is inversely proportional to both the hardness and the fracture toughness of the material.

### ***10.3.4 Chemical (Corrosive) Wear***

In chemical (corrosive) wear, chemical or electrochemical reactions accelerate the wear process [11, 17, 18]. Oxidative wear is a chemical wear process that is observed in many metals. Oxidative wear involves the continuous removal of oxide layers from the contact surface [11]. The removal of material commonly results from sliding contact. After the oxide layer is removed, the denuded metal surface is exposed to air or biological fluids and is quickly reoxidized. As a result, a metal oxide layer re-forms on the surface of the material. These regrown oxide layers are removed by sliding cycles and are subsequently regenerated by exposure to air or biological fluids. It is interesting to note that in many cases the metal oxide may exhibit lower wear rates than the corresponding metal [19]. In other cases, the oxide layer may

**Fig. 10.4** Schematic illustration of oxidative wear behavior



delaminate due to sliding movement if adhesion between the oxide layer and the underlying metal is poor (Fig. 10.4) [17, 18]. Oxidative wear is commonly observed in dry wear processes; it may also be observed in lubricated wear processes. The oxidative wear rate is proportional to  $\exp.[-Q/(R_g T)]$ , where  $T$  is temperature,  $Q$  is the activation energy, and  $R_g$  is the gas constant. This relationship is valid for both metallic and ceramic materials [7].

## 10.4 Wear in Biomedical Devices and Biomaterials

### 10.4.1 Wear in Prostheses and Biomedical Devices

Over the past 40 years, biotribologists have made several notable efforts to increase the wear resistance of prostheses and medical devices. As mentioned earlier, wear may result in the failure of knee joint prostheses, hip joint prostheses, and other orthopedic prostheses [1–3]. Wear may also cause failure of cardiovascular devices, including artificial heart valves [4].

Many efforts have been made to improve the wear resistance of small and large joint prostheses, including shoulder, hip, knee, and finger joints. For example, hip prostheses are utilized for reduction of pain and reestablishment of function in patients who suffer from osteoarthritis, rheumatoid arthritis, osteonecrosis, post-traumatic arthritis, bone tumors, and hip fractures. A large number of hip prosthesis failures are due to osteolysis and aseptic loosening (loosening of the prosthesis-bone interface in the absence of infection). According to a recent National Institutes of Health report, the biological response due to wear debris, along with fixation of the acetabular component and problems associated with revision surgery, is a critical issue that affects life span of hip prostheses [1]. In recent years, the materials and processes used for acetabular fixation have been significantly improved. Unfortunately, osteolysis and other reactions to wear debris remain critical issues that significantly limit the life span of hip prostheses.



A total hip joint prosthesis is composed of a femoral component and an acetabular component. Metals, ceramics, and polymers may be used to fabricate the acetabular component; metals and ceramics may be used to fabricate the femoral components. In a joint prosthesis, four different modes of wear behavior may be observed [12]. Mode 1 wear is associated with articulation between the anticipated bearing surfaces; for example, mode 1 wear in a total hip replacement prosthesis occurs between the femoral head and the acetabular cup. Mode 2 involves articulation between a primary bearing surface and an unintended surface. In a total hip replacement prosthesis, mode 2 wear may take place between the femoral head and the metal backing of the acetabular cup. Mode 3 is a three-body wear process that involves the intended bearing surfaces. Interaction between metal debris, the femoral head, and the acetabular cup is an example of three-body wear. Mode 4 is an articulation between two nonbearing secondary surfaces in a prosthesis.

In a joint prosthesis, the wear rate is dependent on various factors, including the type of motion that takes place when the prosthesis components interact and the number of cycles of motion that the prosthesis undergoes. In addition, wear rate in the artificial joint is also related to the clinical practices, design considerations, patient-specific factors, materials parameters, surface preparation, and tissue-material interaction [5].

The major wear mechanisms for joint prostheses include adhesive, abrasive, fatigue, and corrosive mechanisms [1]. In most situations, wear damage of an implanted device is caused by a combination of these mechanisms, with one or more of these mechanisms being dominant. In metal-polyethylene joint implants, adhesive wear is a common primary wear mechanism.

In joint prostheses that contain metallic and polymeric components, most adhesive wear debris is made up of the softer polymeric material. In many cases, adhesive wear may be correlated with the types of asperities or regions of unevenness on the surface of metal component. Adhesion or cold welding may occur at the asperity-asperity junction regions due to large local stresses. As a result, small pieces of polyethylene are transferred from the polymer to the metal due to junction formation-destruction-reformation process. The wear debris may be either temporarily or permanently attached to the counterface material. The wear volume is proportional to both the sliding distance and the load acting on the device; the wear volume is also inversely proportional to the hardness of the material. The removal of polyethylene results in pitting and void formation on the polyethylene surface.

Asperities on the surface of the metal component can cause abrasive wear of polyethylene. In general, materials that exhibit higher hardness values generally demonstrate higher resistance to abrasive wear. In joint prostheses that contain metallic and polymeric components, abrasive wear damage mostly occurs on the polymer; some damage may also be observed on the metal surface. Two-body abrasive wear in metal-polymer joint prostheses is related to the surface roughness of the metallic component. Scratches on the metal surface may significantly increase the wear rate of the polyethylene surface. Hard particles (e.g., bone cement) may contribute to three-body wear of joint prostheses. These loose particles come from the prosthesis or from the immediate implant-tissue environment. Particles are either

trapped between the contact surfaces (three-body wear) or attached to one of the contact surfaces (two-body wear). Metal, polymer, or bone particles embedded in a polyethylene-bearing surface may induce three-body wear in artificial joints. The rate of abrasive wear is determined by the surface roughness of the metal component and the presence of third-body particles.

Fatigue wear primarily takes place on the softer polyethylene surface. Subsurface delamination and cracking of the polyethylene component may result in the generation of polyethylene debris. Deep cracks in the polymeric biomaterial may result in the formation of particles. Corrosive wear may result from chemical or electrochemical interactions on the prosthesis surface; for example, metals may react with oxygen to form metal oxides on a metallic implant surface. This metal oxide surface may have lower shear strength than the underlying metal and may exhibit a more rapid wear rate. The corrosive wear rate depends on the reactivity of the component materials and the biological environment.

#### ***10.4.2 Wear Resistance of Biomedical Materials***

The materials currently used in total hip joint prostheses include metals, ceramics, and polymers. Two types of polymers are widely used for manufacturing joint devices [20]. For example, ultrahigh molecular weight polyethylene is commonly used for fabricating the liner of the acetabular cup in total hip joint prostheses. Polymethyl methacrylate is a bone cement that is used for attaching (fixing) the hip prosthesis to the surrounding bone. Degradation of both of these polymers may lead to failure of hip prostheses.

Polyethylene contains long chains of ethylene molecules ( $C_2H_4$ ). Ultrahigh molecular weight polyethylene exhibits a molecular weight of 2–6 million g/mole and a melting point of 140–145 °C. The density of ultrahigh molecular weight polyethylene is  $\sim 0.930$ – $0.945$  g/cm<sup>3</sup>, which is similar to the density of high-density polyethylene ( $0.952$ – $0.965$  g/cm<sup>3</sup>) [21, 22]. The mechanical properties of ultrahigh molecular weight polyethylene are dependent on its chemical structure, molecular weight, crystallinity, and thermal history [21].

Ultrahigh molecular weight polyethylene is a semicrystalline polymer that exhibits crystallinity values in range of 45–75% [21–23]. Ultrahigh molecular weight polyethylene consists of 10–50-nm-thick, 10–50- $\mu$ m-long crystalline lamellae, which are surrounded by amorphous regions [21]. The amorphous regions consist of randomly oriented polymer chains that join the lamellae together and impart mechanical strength. The high crystallinity of ultrahigh molecular weight polyethylene provides good resistance to fatigue crack propagation [20]. The crystallinity of ultrahigh molecular weight polyethylene decreases when the material is heated above its melting point; this loss of crystallinity is irreversible [22].

The coefficient of friction for ultrahigh molecular weight polyethylene depends on the counterpart and contact conditions. For example, McKellop et al. reported friction coefficient values from 0.07 to 0.2 for ultrahigh molecular weight

polyethylene lubricated with bovine serum [24]. Similar coefficient of friction results were reported by Klapperich et al.; they reported coefficient of friction values in the range of 0.08–0.23 [23]. The *in vivo* performance of ultrahigh molecular weight polyethylene has also been investigated; average wear rates of ~0.1–0.6 mm/year and wear volumes of 50–100 mm<sup>3</sup>/year were reported by Chiesa et al. [25]. Wear rates for ultrahigh molecular weight polyethylene differ based on the surface properties of the counterpart material. For example, the wear volume of ultrahigh molecular weight polyethylene against cobalt-chromium alloy is ~65 mm<sup>3</sup>/million cycles. On the other hand, the wear rate of ultrahigh molecular weight polyethylene against alumina is 18 mm<sup>3</sup>/million cycles [26, 27].

Every joint prosthesis and implantable medical device must be sterilized prior to implantation. Due to the low thermal tolerance of polyethylene, sterilization is usually performed by exposing the polyethylene component to gamma irradiation at doses between 25 and 40 kGy using a <sup>60</sup>Co source. Irradiation may cause two effects in ultrahigh molecular weight polyethylene, degradation and cross-linking [21, 28–34]. Degradation of ultrahigh molecular weight polyethylene may be caused by oxidation of the material either during irradiation or after device implantation [20, 28, 29]. Oxidation induces the chain scission of ultrahigh molecular weight polyethylene. As a result, the molecular weight of the polymer is reduced, and the mechanical properties of the polymer are altered, resulting in reduced wear resistance. The interaction between high-energy radiation and ultrahigh molecular weight polyethylene results in the formation of free radical species through bond cleavage [35]. The hydrogen radicals produced by C–H bond cleavage have high mobility; on the other hand, the mobility of radicals that result from cleavage of C–C bonds is low. If oxygen is present, free radicals can also form peroxy radicals [28]. Free and peroxy radicals can react with polyethylene chains, resulting in chain scission and additional free radical formation. Newly generated free radical species maintain these reactions and contribute to the degradation of polyethylene. Chain scission reduces the length of polymer chain and increases the crystallinity of the polymer. The reduction of chain length and molecular weight alters the physical properties of ultrahigh molecular weight polyethylene. The density and elastic modulus values of ultrahigh molecular weight polyethylene increase due to the chain scission; as a result, the material becomes brittle. The fatigue, fracture, and wear resistance values for oxidized ultrahigh molecular weight polyethylene are lower than those for as-prepared material. Free radical species demonstrate very long lifetimes. Even if radiation sterilization of ultrahigh molecular weight polyethylene is performed in an oxygen-free environment, free radical species may be formed that cause embrittlement of the material. Oxidative degradation may continue after the prostheses are implanted in the body; this degradation process may result in poor long-term wear resistance.

Free radicals created during high-energy irradiation may be minimized using thermal processes, including annealing or melting processes [34]. Unfortunately, these treatments are not practical for total joint prostheses and other medical devices. Several attempts have been made to increase the wear resistance of ultrahigh molecular weight polyethylene [21]. One possibility involves the use of carbon

fiber-reinforced ultrahigh molecular weight polyethylene (Poly II™). This composite material contains short carbon fibers in an ultrahigh molecular weight polyethylene matrix. Although laboratory studies provided promising results for this composite, *in vivo* implantation studies demonstrated osteolysis and mechanical failure [21, 36–38]. It was found that the carbon fiber-reinforced composite exhibited very low crack resistance compared with ultrahigh molecular weight polyethylene, since the carbon fiber did not bond to the polymer matrix [21].

Cross-linking is an effective method for improving the abrasive wear resistance of polyethylene [21, 39–41]. Cross-linking of polyethylene chains may be performed using three different methods: irradiation, peroxide chemistry, and silane chemistry [21]. In the irradiation method, gamma ray or other radiation is used to cleave C–H and C–C bonds in polyethylene in order to produce free radicals. The molecular weight of the polymer is reduced when carbon-carbon bonds are cleaved (chain scission). Cross-linking is achieved when interchain covalent bonds are formed by the reaction of free radicals from different chains. If cross-linking involves radicals from C–H bonds, it is referred to as H-type cross-linking. Y-type cross-linking results from reactions between the free radicals generated by the cleavage of C–C bonds. Cross-linking is most significant in amorphous regions of ultrahigh molecular weight polyethylene. Improvements in the physical properties of ultrahigh molecular weight polyethylene are dependent on several cross-linking parameters, including technique, dose, radiation source, process temperature, and process time. Cross-linking may significantly improve the wear resistance of ultrahigh molecular weight polyethylene; however, the fracture toughness of cross-linked ultrahigh molecular weight polyethylene may be reduced [34].

Metal-on-metal joint prostheses have been developed in an attempt to reduce the number of total hip joint prosthesis failures associated with wear of ultrahigh molecular weight polyethylene. Early metal-on-metal hip prosthesis designs were fabricated using stainless steel; however, most current metal-on-metal hip prostheses contain two components that are fabricated out of cobalt-chromium alloys [42, 43]. First-generation metal-on-metal prostheses were replaced with ultrahigh molecular weight polyethylene/cobalt-chromium alloy prostheses in the 1970s for several reasons, including seizure of the cast metal surfaces [42, 43]. Second-generation cobalt-chromium alloy/cobalt-chromium alloy prostheses were developed in the 1980s. During *in vivo* studies, these implants demonstrated a 1-year “running-in” period, in which the wear rate of 25  $\mu\text{m}/\text{year}$  was observed. After the “running-in” period, a more impressive *in vivo* wear rate of 5  $\mu\text{m}/\text{year}$  was noted. Abrasive wear is the dominant wear mechanism for these devices; however, adhesive wear and fatigue wear have also been observed.

Ceramic materials have been used in joint prostheses as an alternative to the polyethylene-metal design since the 1970s [44]. The two most common ceramic materials used in prosthesis bearing surfaces are alumina and zirconia. Alumina exhibits very high hardness (Vickers hardness 400–450 GPa) and elastic modulus (380 GPa) values [45]. Prostheses containing alumina components generally produce a low number of wear particles. A wear rate of 0.1  $\text{mm}^3/\text{million cycles}$  has been reported for alumina-on-alumina devices; this value is significantly lower than

the wear rate that has been reported for cobalt-chromium alloy-polyethylene devices ( $65 \text{ mm}^3/\text{million cycles}$ ) [26, 27]. Several factors may contribute to the enhanced wear resistance of alumina. In addition to the high hardness, alumina components can be manufactured with very low surface roughness ( $<0.005 \mu\text{m}$ ); as a result, abrasive wear is minimized. The hydrophilic nature of alumina may also contribute to good wear resistance properties, since it enables full film lubrication [46]. One major drawback of alumina is low fracture toughness values (brittleness), which can cause failure of the prosthesis or medical device [44].

Zirconia (zirconium oxide,  $\text{ZrO}_2$ ) exhibits higher fracture toughness values than alumina. Pure zirconia has three different crystalline phases: cubic, tetragonal, and monoclinic. At room temperature, pure zirconia is monoclinic. The transformation from the monoclinic phase to the tetragonal phase occurs at  $1000\text{--}1100 \text{ }^\circ\text{C}$ . At  $2000 \text{ }^\circ\text{C}$ , transformation from the tetragonal phase to the cubic phase takes place. Shape change and volume expansion are associated with each phase transformation. The stresses created by these phase transformations result in the formation of cracks. For this reason, zirconia is stabilized with yttrium oxide ( $\text{Y}_2\text{O}_3$ ) or magnesium oxide ( $\text{MgO}$ ); these doped structures exhibit a stable tetragonal phase at room temperature. Doped zirconia materials include partially stabilized zirconia (PSZ), tetragonal zirconia polycrystals (TZP), and zirconia toughened ceramics. For example, yttrium-stabilized tetragonal zirconia polycrystal material is a fine-grained material that exhibits high fracture toughness values ( $6\text{--}12 \text{ MPa m}^{1/2}$ ); these values are approximately twice as high as that of alumina ( $4\text{--}5 \text{ MPa m}^{1/2}$ ) [44]. However, yttrium-stabilized tetragonal zirconia polycrystals undergo a slow transformation from tetragonal to monoclinic phase. Sato et al. have shown that water molecules in the environment promote the tetragonal-monoclinic transformation on the surface of zirconia prostheses [47]. This volume change leads to surface microcrack formation, which can result in an increase in surface roughness.

Surface modification has been considered for optimizing the wear resistance and biocompatibility of the total hip joint prostheses and other medical devices [48]. For example, superhard biocompatible coatings, including titanium nitride, silicon carbide, tungsten carbide, and diamond-like carbon, have been utilized for increasing the wear and corrosion resistance of metallic biomaterials [49]. Diamond-like carbon is a metastable amorphous material that contains both  $\text{sp}^3$ -hybridized carbon atoms and  $\text{sp}^2$ -hybridized carbon atoms; hydrogenated and nonhydrogenated forms of this material may be prepared. Diamond-like carbon is a superhard material. The elastic modulus and hardness value of diamond-like carbon depend on the fraction of  $\text{sp}^3$ -hybridized atoms in the films [50–53]. An  $\text{sp}^3$  fraction of 10% corresponds to a hardness value of  $2000\text{--}3000 \text{ Hv}$ . As the fraction of  $\text{sp}^3$ -hybridized carbon atoms increases to 50%, a hardness value of  $7000\text{--}8000 \text{ Hv}$  can be achieved. Diamond-like carbon films with 100%  $\text{sp}^3$ -hybridized carbon atoms have demonstrated hardness values of  $10,000 \text{ Hv}$  [54]. The elastic modulus values for diamond-like carbon films with 0% to 90%  $\text{sp}^3$ -hybridized carbon atoms can vary between  $300 \text{ GPa}$  and  $800 \text{ GPa}$  [55].

The coefficients of friction values for diamond-like carbon coatings depend on the amount of hydrogen incorporated in the film, ambient humidity, topology, and

sliding partner [56]. For example, humidity plays a significant role in determining the coefficient of friction for hydrogenated diamond-like carbon coatings. The coefficient for hydrogenated diamond-like carbon coatings is in the range of 0.01–0.3 in vacuum conditions, but it greatly increases under humid conditions. On the other hand, hydrogen-free diamond-like carbon coatings demonstrate low coefficient of friction values ( $<0.1$ ) under both low and high humidity conditions [57].

Diamond-like carbon coatings can significantly improve wear resistance of metallic biomaterials. For example, Affatato et al. performed an *in vitro* investigation of femoral heads coated with diamond-like carbon [48]. In their study, diamond-like carbon was coated on a titanium alloy (Ti6Al4V) head using chemical vapor deposition. They found that wear of the polyethylene-diamond-like carbon-coated Ti6Al4V couple was comparable to that of the polyethylene-alumina couple. Similar results have been reported by other groups for diamond-like carbon-coated cobalt-chromium-molybdenum alloy-polyethylene and diamond-like carbon-coated stainless steel-polyethylene devices [58, 59]. However, there is some controversy in the reported results. For example, Sheeja et al. indicated there was only a slight difference in wear rates between cobalt-chromium-molybdenum alloy-ultrahigh molecular weight polyethylene and multilayered diamond-like carbon-coated cobalt-chromium-molybdenum alloy-ultrahigh molecular weight polyethylene wear couples [60].

The major problem associated with diamond-like carbon coatings on metal surfaces is poor adhesion, which is related to compressive stress in the film and poor chemical bonding between the film and the substrate [61, 62]. The internal compressive stress within diamond-like carbon coatings can be as high as 10 GPa, which limits the coating thickness in range 100–200  $\mu\text{m}$ . To reduce film stress and increase film thickness, diamond-like carbon-metal composite coatings have been utilized. Diamond-like carbon-metal composite coatings, including diamond-like carbon-silver composite coatings and diamond-like carbon-titanium composite coatings, maintain hardness and wear properties similar to those of unalloyed diamond-like carbon films. In addition, they exhibit excellent adhesion to medical alloy substrates [63, 64].

## 10.5 Summary

The wear properties of biomedical materials play a major role in determining the overall success of medical prostheses and other implantable medical devices. Adhesive wear, abrasive wear, fatigue wear, and corrosive wear play a key role in degradation of medical devices and prostheses. Several factors determine the relationship between the *in vitro* properties of the component materials and the *in vivo* wear performance of the medical device or prosthesis. Significant improvements in the wear properties of biomedical materials may be achieved through intensive examination of material-, device-, surgical-, and patient-specific parameters that

determine in vivo wear behavior. Minimization of wear in biomedical materials may only be achieved through effective interaction among clinicians, biotribologists, and biologists.

## References

1. Wright TM, Goodman SB, editors. *Implant wear in total joint replacement: clinical and biologic issues, material and design considerations*. Rosemont: American Academy of Orthopaedic Surgeons; 2001.
2. Zhu YH, Chiu KY, Tang WM. Polyethylene wear and osteolysis in total hip arthroplasty. *J Orthop Surg*. 2001;9:91–9.
3. Teoh SH. Fatigue of biomaterials: a review. *Int J Fatigue*. 2000;22:825–37.
4. Kelpetko V, Moritz A, Schurawitzki H, Domanig E, Wolner E. Leaflet fracture in Edwards–Duromedics bileaflet valves. *J Thorac Cardiovasc Surg*. 1989;97:90–4.
5. Hutchings IM, editor. *Biotribology – a personal view, friction, lubrication and Wear of artificial joints*. Bury St. Edmunds: Professional Engineering Publishing Ltd; 2003.
6. Buckley DH, Jones WR Jr, Sliney HE, Zaretsky EV, Townsend DP, Loewenthal SH. *Tribology: the story of lubrication and wear*. NASA technical memorandum 101430, 1985.
7. Behushan B, editor. *Modern tribology handbook*. Boca Raton: CRC Press; 2001.
8. Black J. *Biological performance of materials: fundamentals of biocompatibility*. New York: Marcel Dekker; 1992.
9. Standard terminology relating to wear and erosion, standard G-40-01, American Society for Testing and Materials, 2001.
10. Hutchings IM. The challenge of wear. In: Stachowiak GW, editor. *Wear-materials, mechanisms and practice*: Chichester, England. Hoboken: Wiley; 2005., Chapter 1. p. 1–7.
11. Bayer RG. *Mechanical wear: fundamentals and testing*. New York: Marcel Dekker Inc.; 2004.
12. McKellop HA. The lexicon of polyethylene wear in artificial joints. *Biomaterials*. 2007;28:5049–57.
13. Stachowiak GW, Batchelor AW. *Engineering tribology*. Amsterdam: Elsevier Butterworth-Heinemann; 2005.
14. Buckley DH, Miyoshi K. Friction and wear of ceramics. *Wear*. 1984;100:333–53.
15. Archard JF. Contact and rubbing of flat surfaces. *J Appl Phys*. 1953;24:981–8.
16. Burwell JT Jr. Survey of possible wear mechanisms. *Wear*. 1957;1:119–41.
17. Burwell JT, Strang CD. On the empirical law of adhesive wear. *J Appl Phys*. 1952;23:18–28.
18. Rabinowicz E. *Adhesive wear. Friction and wear of materials*. New York: Wiley; 1965.
19. Bhushan B, Gupta B. *Handbook of tribology*. Section 3.3. New York: McGraw-Hill; 1991.
20. Santavirta S, Kontinen YT, Lappalainen R, Anttila A, Goodman SB, Lind M, Smith L, Takagi M, Gdmez-Barrena E, Nordstletten L, Xu J-W. *Materials in total joint replacement*. *Curr Orthop*. 1998;12:51–7.
21. Kurtz SM, Muratoglu OK, Evans M, Edidin AA. Advances in the processing, sterilization, and crosslinking of ultra-high molecular weight polyethylene for total joint arthroplasty. *Biomaterials*. 1999;20:1659–88.
22. Li S, Burstein AH. Ultra high molecular weight polyethylene. The material and its use in total hip joint implants. *J Bone Joint Surg Am*. 1994;76:1080–90.
23. Klapperich C, Komvopoulos K, Pruitt L. Tribological properties and microstructure evolution of ultra-high molecular weight polyethylene. *Trans ASME*. 1999;121:394–402.
24. McKellop H, Clarke IC, Markolf KL, Amstutz HC. Wear characteristics of UHMW polyethylene: a method for accurately measuring extremely low wear rates. *J Biomed Mater Res*. 1978;12:895–927.

25. Chiesa R, Tanzi MC, Alfonsi S, Paracchini L, Moscatelli M, Cigada A. Enhanced wear performance of highly crosslinked UHMWPE for artificial joints. *J Biomed Mater Res A*. 2000;50:381–7.
26. Buford A, Goswami T. Review of wear mechanisms in hip implants: paper I – general. *Mater Des*. 2004;25:385–93.
27. Buford A, Goswami T. Review of wear mechanisms in hip implants: paper II – ceramics IG004712. *Mater Des*. 2004;25:385–93.
28. Daly BM, Yin J. Subsurface oxidation of polyethylene. *J Biomed Mater Res*. 1998;42:523–9.
29. Goldman M, Lee M, Gronsky R, Pruitt L. Oxidation of ultrahigh molecular weight polyethylene characterized by Fourier transform infrared spectrometry. *J Biomed Mater Res*. 1997;37:43–50.
30. Lee CS, Yoo SH, Jho JY. Mechanical properties of ultra-high molecular weight polyethylene irradiated with gamma rays. *Macromol Res*. 2004;12:112–8.
31. Rose RM, Goldfarb EV, Ellis E, Crugnola AN. Radiation sterilization and the wear rate of polyethylene. *J Orthop Res*. 1984;2:393–400.
32. Goldman M, Pruitt L. Comparison of the effects of gamma radiation and low temperature hydrogen peroxide gas plasma sterilization on the molecular structure, fatigue resistance, and wear behavior of UHMWPE. *J Biomed Mater Res*. 1998;40:378–84.
33. McKellop H, Shen F-W, Lu B, Campbell P, Salovey R. Effect of sterilization method and other modifications on the wear resistance of acetabular cups made of ultra-high molecular weight polyethylene. *J Bone Joint Surg*. 2000;82:1708–25.
34. Maher SA, Furman BD, Babalola OM, Cottrell JM, Wright TM. Effect of crosslinking, remelting, and aging on UHMWPE damage in a linear experimental wear model. *J Orthop Res*. 2007;25:849–57.
35. Bracco P, Brunella V, Luda MP, Zanetti M, Costa L. Radiation-induced crosslinking of UHMWPE in the presence of co-agents: chemical and mechanical characterisation. *Polymer*. 2005;46:10648–57.
36. Wright TM, Bartel DL. The problem of surface damage in polyethylene total knee components. *Clin Orthop*. 1986;205:67–74.
37. Wright TM, Astion DJ, Bansal M, Rinnac CM, Green T, Insall JN, Robinson RP. Failure of carbon fiber-reinforced polyethylene total knee-replacement components. A report of two cases. *J Bone Joint Surg A*. 1988;70:926–32.
38. Wright TM, Rinnac CM, Faris PM, Bansal M. Analysis of surface damage in retrieved carbon fiber-reinforced and plain polyethylene tibial components from posterior stabilized total knee replacements. *J Bone Joint Surg A*. 1988;70:1312–9.
39. Heisel C, Silva M, Dela Rosa MA, Schmalzried TP. Short-term in vivo wear of cross-linked polyethylene. *J Bone Joint Surg Am*. 2004;86:748–51.
40. Dorr LD, Wan Z, Shahrdar C, Sirianni L, Boutary M, Yun A. Clinical performance of a duralul highly cross-linked polyethylene acetabular liner for total hip arthroplasty at five years. *J Bone Joint Surg Am*. 2005;87:1816–21.
41. Martell JM, Verner JJ, Incavo SJ. Clinical performance of a highly cross-linked polyethylene at two years in total hip arthroplasty: a randomized prospective trial. *J Arthroplast*. 2003;18:55–9.
42. Steinberg DR, Steinberg ME. The early history of arthroplasty in the United States. *Clin Orthop Relat Res*. 2000;374:55–89.
43. Rieker CB, Köttig P, Schön R, Windler M, Wyss UP. Clinical wear performance of metal-on-metal hip arthroplasties. In: Jacobs JJ, Craig TL, editors. *Alternative bearing surfaces in Total joint replacement*. West Conshohocken: ASTM International; 1998.
44. Rahaman MN, Yao A, Bal BS, Garino JP, Ries MD. Ceramics for prosthetic hip and knee joint replacement. *J Am Ceram Soc*. 2007;90:1965–88.
45. Boutin P, Christin P, Dorlot JM, Meunier A, de Roquancourt A, Blanquaert D, Herman S, Sedel L, Witvoet J. The use of dense alumina-alumina ceramic combination in total hip replacement. *J Biomed Mater Res*. 1988;22:1203–32.



46. Hutchings IM, editor. Friction, lubrication and Wear of artificial joints. Bury St. Edmunds: Professional Engineering Publishing Ltd.; 2003.
47. Sato T, Ohtaki Y, Endo T, Shimada M. Science and technology of zirconia. In: Somiya S, Yamamoto N, Yanagida H, editors. *Advances in Ceramics*. Westerville: American Ceramic Society; 1988.
48. Affatato S, Frigo M, Toni A. An in vitro investigation of diamond-like carbon as a femoral head coating. *J Biomed Mater Res (Appl Biomater)*. 2000;53:221–6.
49. Dearnaley PA. A review of metallic, ceramic and surface treated metals used for bearing surfaces in human joint replacements. *Proc Inst Mech Eng*. 1999;213-H:107–35.
50. Enke K, Dimigen H, Hubsch H. Frictional properties of diamond-like carbon layers. *Appl Phys Lett*. 1980;36:291–2.
51. Pharr GM, Callahan DL, McAdams SD, Tsui TY, Anders S, Anders A, Ager JW, Brown IG, Bhatia CS, Silva SRP, Robertson J. Hardness, elastic modulus, and structure of very hard carbon films produced by cathodic-arc deposition with substrate pulse-biasing. *Appl Phys Lett*. 1996;68:779–81.
52. Ronkainen H, Varjus S, Koskinen J, Holmberg K. Differentiating the tribological performance of hydrogenated and hydrogen-free DLC coatings. *Wear*. 2001;249:260–6.
53. Holmberg K, Mathews A. Coatings tribology: a concept, critical aspects, and future directions. *Thin Solid Films*. 1994;253:173–8.
54. Collins CB, Davanloo F, Lee TJ, Park H, You JH. Noncrystalline films with the chemistry, bonding, and properties of diamond. *J Vac Sci Technol B*. 1993;11:1936–41.
55. Schneider D, Schwarz T, Scheibe HJ, Panzner M. Non-destructive evaluation of diamond and diamond-like carbon films by laser induced surface acoustic waves. *Thin Solid Films*. 1997;295:107–16.
56. Erdemir A, Bindal C, Pagan J, Wilbur P. Characterization of transfer layers on surfaces sliding against diamond-like hydrocarbon films in dry nitrogen. *Surf Coat Technol*. 1995;76–77:559–63.
57. Liu Y, Erdemir A, Meletis EI. An investigation of the relationship between graphitization and frictional behavior of DLC coatings. *Surf Coat Technol*. 1996;86:564–8.
58. Lappalainen R, Heinonen H, Anttila A, Santavirta S. Some relevant issues related to the use of amorphous diamond coatings for medical applications. *Diamond Relat Mater*. 1998;7:482–5.
59. Dearnaley G, Mccabe A. Bioapplications of diamond-like carbon coatings. 4th World Biomater Cong, Berlin; 1992.
60. Sheeja D, Tay BK, Lau SP, Nung LN. Tribological characterization of diamond-like carbon coatings on co-Cr-Mo alloy for orthopaedic applications. *Surf Coat Technol*. 2001;146:410–6.
61. Morshed MM, McNamara BP, Cameron DC, Hashmi MSJ. Effect of surface treatment on the adhesion of DLC film on 316L stainless steel. *Surf Coat Technol*. 2003;163:541–5.
62. Schwan J, Ulrich S, Theel T, Roth H, Ehrhardt H, Becker P, Silva SRP. Stress-induced formation of high-density amorphous carbon thin films. *J Appl Phys*. 1997;82:6024–30.
63. Morrison ML, Buchanan RA, Liaw PK, Berry CJ, Brigmon R, Riester L, Jin C, Narayan RJ. Electrochemical and antimicrobial properties of diamond-like carbon-metal composite films. *Diamond Relat Mater*. 2006;15:138–46.
64. Bell BF, Scholvin D, Jin C, Narayan RJ. Pulsed laser deposition of hydroxyapatite-diamond-like carbon multilayer films and their adhesion aspects. *J Adhes Sci Technol*. 2006;18:221–32.